Available online at www.sciencedirect.com

ScienceDirect

IFAC PapersOnline CONFERENCE PAPER ARCHIVE

IFAC PapersOnLine 54-21 (2021) 19–24

Disturbance Propagation Through a Grinding-Flotation Circuit

D. A. Wepener * **J. D. le Roux** *,1 **I. K. Craig** *

* *Department of Electrical, Electronic and Computer Engineering, University of Pretoria, Pretoria, South Africa*

Abstract: The propagation of common disturbances in a grinding circuit connected to a flotation circuit and the effects of these disturbances on flotation cell levels were simulated and analysed. The disturbances include changes in the mineral ore feed as well as a step change in the cyclone operating condition and spillage water added to the sump. The effect of the disturbances on the cell levels remains relatively small, but it is clear that multivariable control is required to prevent the propagation of the disturbances through the cells. The simulation of a grinding-flotation circuit is useful to simulate the effects of disturbance propagation and will be helpful when designing plant-wide controllers.

Copyright © 2021 The Authors. This is an open access article under the CC BY-NC-ND license (https://creativecommons.org/licenses/by-nc-nd/4.0/)

Keywords: Grinding-flotation circuit, disturbance propagation, flotation level control, plant-wide control, mineral processing, flotation, grinding

1. INTRODUCTION

Mineral processing refers to the chain of processes used to transform raw ore into a final product that can be used for industrial or commercial applications. The chain that will be used in this study consists of two main stages, the grinding stage and the flotation stage. The grinding-flotation circuit has been used for a long time to extract valuable minerals from ore. Although many advancements have been made to make the process more efficient, there is still room for improvement. According to Hodouin et al. (2001), plant-wide economic optimisation is the only final goal of the mineral processing industry. In plant-wide control, the grinding and flotation circuits are controlled together to optimise some operational objective of the entire plant instead of separate objectives for the circuits (le Roux and Craig, 2019).

Before optimal plant-wide controllers for a grinding-flotation circuit can be designed, it is important to understand the effect that the grinding circuit has on the flotation circuit. Mineral liberation is the most important property of the grinding circuit and has the largest impact on the flotation circuit (McIvor and Finch, 1991; Schena et al., 1996; Sosa-Blanco et al., 2000; Muñoz and Cipriano, 1999; Wei and Craig, 2009a; Thivierge et al., 2019). The effect of disturbance propagation from the grinding circuit to the flotation circuit is an important property to consider when designing a plant-wide controller.

The aim of this paper is to analyse the effect of different common disturbances in a grinding circuit on the levels of flotation cells to identify plant-wide control challenges. Since few plant-wide simulation platforms for mineral processing plants exist, the contribution of this paper is to present a simple simulation framework of a grinding mill circuit combined with a flotation circuit. A description of the mineral processing process is given in section 2. The grinding and flotation circuit models are described in sections 3 and 4. The simulation setup and results are shown in section 5 and discussed in section 6.

2. PROCESS DESCRIPTION

The considered single-stage closed run-of-mill (ROM) ore grinding circuit includes three main components: a semi-autogenous (SAG) grinding mill, a sump and a hydrocyclone. The grinding mill is responsible for liberating the ore down to small particles. The mined ore flows into the mill along with water and the underflow of the hydrocyclone. Inside the mill steel balls and large rocks (grinding media) are used to break down the ore into ore material that mixes with the water to form a slurry. A motor rotates the mill causing the charge in the mill to be lifted by the inner liners and can become airborne before crashing down to the bottom of the mill. An end-discharge-screen allows some of the slurry to discharge from the mill, separating the rocks and the solids. Solids are defined as ore material small enough to pass through the screen. Rocks are defined as ore too large to be discharged by the mill. Solids can be divided further into coarse and fine ore, where fine ore is all ore smaller than the final product specification size ($75\mu m$), and coarse ore is ore larger than the product specification size. The mill outlet is mixed with water in the sump and then pumped to the hydrocyclone. The cyclone classifies the material into light small particles and heavy large particles. The small particles pass to the overflow and then on to the flotation circuit and the large particles pass via the underflow back to the mill (Wei and Craig, 2009b).

Flotation uses the hydrophobicity property of the different particles in the mineral ore by separating the hydrophobic particles from the hydrophilic particles in a three-phase system (Jovanović and Miljanović, 2015). The three phases refer to the mineral particles (solid), water (liquid) and air (gas) that interact with each other inside a flotation tank.

[1] Corresponding author, E-mail: derik.leroux@up.ac.za

2405-8963 Copyright © 2021 The Authors. This is an open access article under the CC BY-NC-ND license.
Peer review under responsibility of International Federation of Automatic Control.
10.1016/j.ifacol.2021.12.004

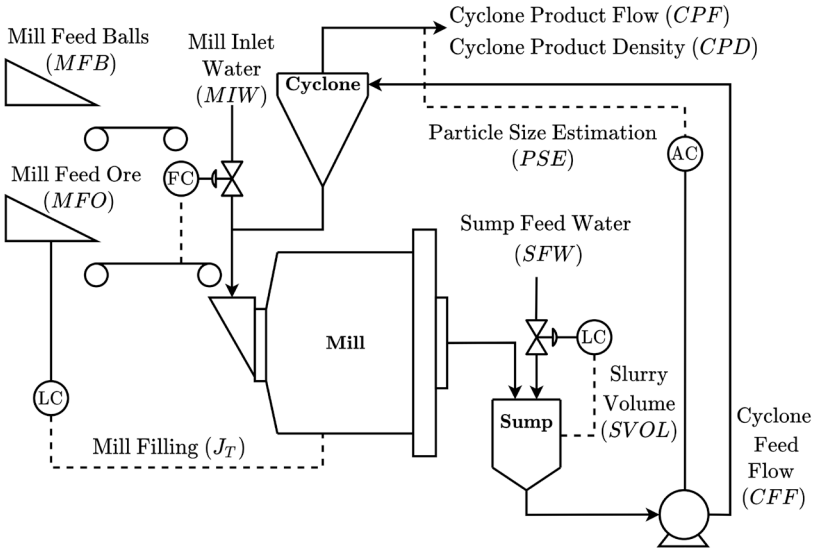

Fig. 1. Grinding circuit configuration with regulatory controllers

Some minerals are not naturally hydrophobic, in which case chemicals called collectors are added to the slurry to improve the hydrophobicity properties. Other reagents can also be added to stabilise the foams in the froth phase (frothers) or to modify other chemical properties to optimise the process (modifiers). The aim of the flotation process is for the valuable mineral particles to attach to air bubbles introduced in the flotation tank and flow to the top of the tank while the gangue flows to the bottom. In industry, flotation tanks are connected in flotation banks and each bank has a specific function in the flotation process. The functions of the flotations banks can be divided into three sections: rougher, scavenger and cleaner banks (Laurila et al., 2002).

3. GRINDING CIRCUIT MODEL DESCRIPTION

The *Hulbert* grinding mill model of le Roux et al. (2013) will be used here to simulate the grinding circuit, and is divided into three modules: mill, sump and hydrocyclone. Fig. 1 shows the configuration of the grinding circuit including the mill, sump and cyclone modules. In the model, the flow-rates in m^3/h are given by Q and the volumetric states in m^3 by V. The first subscript of Q and V indicate the module (**m**ill, **s**ump or **c**yclone). The second subscript specifies the state (**w**ater, **s**olids, **c**oarse, **f**ines, **r**ock, **b**alls or **t**otal). The flow rates have a third subscript that indicates if the flow is an **i**nflow, **o**utflow or **u**nderflow.

3.1 Mill

The changes in the mill states are given by,

$$\dot{V}_{mw} = MIW + Q_{cwu} - Q_{mwo}, \tag{1a}$$

$$\dot{V}_{ms} = \frac{MFO}{\rho_O}(1-\alpha_r) + Q_{csu} - Q_{mso} + Q_{RC}, \tag{1b}$$

$$\dot{V}_{mf} = \frac{MFO}{\rho_O}\alpha_f + Q_{cfu} - Q_{mfo} + Q_{FP}, \tag{1c}$$

$$\dot{V}_{mr} = \frac{MFO}{\rho_O}\alpha_r - Q_{RC}, \tag{1d}$$

$$\dot{V}_{mb} = \frac{MFB}{\rho_B} - Q_{BC}, \tag{1e}$$

where MIW (m^3/h) is the Mill Inlet Water, MFO (t/h) is the Mill Feed Ore, MFB (t/h) is the Mill Feed Balls, ρ_O (t/m^3) is the density of ore, ρ_B (t/m^3) is the density of balls, α_r is the fraction of rock in the ore, and α_f the fraction of fines in the ore. Q_{RC} represents the rock consumption, Q_{BC} is the ball consumption, and Q_{FP} is the fines production in the mill. The mill rheology factor is,

$$\varphi = \begin{cases} \sqrt{1-\left(\varepsilon_0^{-1}-1\right)\frac{V_{ms}}{V_{mw}}} & ; \ \frac{V_{ms}}{V_{mw}} \leq \left(\varepsilon_0^{-1}-1\right)^{-1} \\ 0 & ; \ \frac{V_{ms}}{V_{mw}} > \left(\varepsilon_0^{-1}-1\right)^{-1} \end{cases} \tag{2}$$

where ε_0 is the fraction of solids by volume of slurry. The mill power draw is,

$$P_{mill} = (1 - \delta_{Pv}Z_x^2 - 2\chi_P\delta_{Pv}\delta_{Ps}Z_xZ_r - \delta_{Ps}Z_r^2) \cdot P_{max}(\alpha_{speed})^{\alpha_P}, \tag{3}$$

where P_{max} (kW) is the maximum mill motor power draw, δ_{Pv} is the power-change parameter for volume, δ_{Ps} is the power-change parameter for fraction solids, χ_P is the cross-term for maximum power draw, α_{speed} is the fraction of critical mill speed, and α_P is the fractional power reduction per fractional reduction from maximum mill speed. The effect of the total charge on mill power (Z_x) is,

$$Z_x = \frac{LOAD}{v_{mill} \cdot v_{P_{max}}} - 1, \tag{4}$$

where v_{mill} (m^3) is the total mill volume, $v_{P_{max}}$ is the fraction of the mill filled for maximum power draw and the load in the mill is,

$$LOAD = V_{mw} + V_{mr} + V_{ms} + V_{mb} \tag{5}$$

with the fraction of the mill filled given by,

$$J_T = \frac{LOAD}{v_{mill}}. \tag{6}$$

The effect of the slurry rheology on mill power (Z_r) is,

$$Z_r = \frac{\varphi}{\varphi_{P_{max}}} - 1, \tag{7}$$

where $\varphi_{P_{max}}$ is the rheology factor for maximum mill power draw. The breakage function for rock consumption is,

$$Q_{RC} = \frac{P_{mill} \cdot \varphi}{\rho_O \phi_r} \left(\frac{V_{mr}}{V_{mr} + V_{ms}} \right), \tag{8}$$

where ϕ_r (kWh/t) is the rate of rock consumption in the mill. The breakage function for ball consumption is given by,

$$Q_{BC} = \frac{P_{mill} \cdot \varphi}{\phi_b} \left(\frac{V_{mb}}{\rho_O \cdot (V_{mr} + V_{ms}) + \rho_B \cdot V_{mb}} \right), \tag{9}$$

where ϕ_b (kWh/t) is the rate of ball consumption in the mill. The production of fines in the mill is,

$$Q_{FP} = \frac{P_{mill}}{\rho_O \cdot \left(\phi_f \cdot \left(1 + \alpha_{\phi_f} \cdot \left(\frac{LOAD}{v_{mill}} - v_{P_{max}} \right) \right) \right)}, \tag{10}$$

where ϕ_f (kWh/t) is the power needed per tonne of fines produced, and α_{ϕ_f} is the fractional change in power per fines produced per change in fractional filling of the mill. The discharge flow rates out of the mill are given by,

$$Q_{mwo} = d_q \cdot \varphi \cdot V_{mw} \cdot \left(\frac{V_{mw}}{V_{ms} + V_{mw}} \right), \tag{11a}$$

$$Q_{mso} = d_q \cdot \varphi \cdot V_{mw} \cdot \left(\frac{V_{ms}}{V_{ms} + V_{mw}} \right), \tag{11b}$$

$$Q_{mfo} = d_q \cdot \varphi \cdot V_{mw} \cdot \left(\frac{V_{mf}}{V_{ms} + V_{mw}} \right), \tag{11c}$$

$$Q_{mro} = 0, \tag{11d}$$

$$Q_{mbo} = 0, \tag{11e}$$

where d_q is the discharge constant.

3.2 Mixed-sump

The changes in the sump states are given by,

$$\dot{V}_{sw} = Q_{swi} - Q_{swo} + SFW, \tag{12a}$$

$$\dot{V}_{ss} = Q_{ssi} - Q_{sso}, \tag{12b}$$

$$\dot{V}_{sf} = Q_{sfi} - Q_{sfo}, \tag{12c}$$

where SFW (m^3/h) is the Sump Feed Water and the input flow rates to the sump is equal to the mill output flow rates given by,

$$Q_{swi} = Q_{mwo}, \tag{13a}$$

$$Q_{ssi} = Q_{mso}, \tag{13b}$$

$$Q_{sfi} = Q_{mfo}. \tag{13c}$$

The Cyclone Feed Density (t/m^3) is,

$$CFD = \frac{V_{sw} + \rho_O \cdot V_{ss}}{SVOL}, \tag{14}$$

where the volume of slurry in the sump is,

$$SVOL = V_{sw} + V_{ss}. \tag{15}$$

The sump discharge flow-rates are given by,

$$Q_{swo} = CFF \cdot \left(\frac{V_{sw}}{SVOL} \right), \tag{16a}$$

$$Q_{sso} = CFF \cdot \left(\frac{V_{ss}}{SVOL} \right), \tag{16b}$$

$$Q_{sfo} = CFF \cdot \left(\frac{V_{sf}}{SVOL} \right), \tag{16c}$$

where CFF is the cyclone feed flow rate.

3.3 Hydrocyclone

The cyclone coarse ore underflow is,

$$Q_{ccu} = \left(1 - C_1 e^{\left(\frac{-CFF}{\varepsilon_c} \right)} \right) \left(1 - \left(\frac{F_i}{C_2} \right)^{C_3} \right) \left(1 - P_i^{C_4} \right) (Q_{sso} - Q_{sfo}), \tag{17}$$

where ε_c (m^3/h) is a parameter related to coarse split, $F_i = \frac{Q_{sso}}{CFF}$, $P_i = \frac{Q_{sfo}}{Q_{sso}}$ and C_1, C_2, C_3 and C_4 are constant cyclone parameters. The underflow of water and fines are given by,

$$Q_{cwu} = \frac{Q_{swo}(Q_{ccu} - F_u Q_{ccu})}{F_u Q_{swo} + F_u Q_{sfo} - Q_{sfo}} \tag{18a}$$

$$Q_{cfu} = \frac{Q_{sfo}(Q_{ccu} - F_u Q_{ccu})}{F_u Q_{swo} + F_u Q_{sfo} - Q_{sfo}}, \tag{18b}$$

where

$$F_u = 0.6 - (0.6 - F_i) \cdot e^{\left(\frac{-Q_{ccu}}{\alpha_{su} \varepsilon_c} \right)} \tag{19}$$

and α_{su} is the fraction of solids in the underflow. The outflow flow rates can be determined by subtracting the underflows from the inflows. The Cyclone Product Flow (CPF) (m^3/h), product Particle Size Estimation (PSE) (fraction of fines in the product) and Cyclone Product Density (CPD) (t/m^3) are given by,

$$CPF = Q_{cwo} + Q_{cso} \tag{20a}$$

$$PSE = \frac{Q_{cfo}}{Q_{cco} + Q_{cfo}} \tag{20b}$$

$$CPD = \frac{Q_{cso}\rho_O + Q_{cwo}}{CPF}. \tag{20c}$$

3.4 Grinding Circuit Parameters

Table 1 shows the plant data obtained from an industrial milling circuit and Table 2 shows the estimated model parameters for the *Hulbert* model and the initial states.

Table 1. Grinding circuit plant data.

Parameter	Value	Unit	Parameter	Value	Unit
MIW	373	m^3/h	V_{mill}	497	m^3
MFO	759	t/h	J_T	0.307	–
α_r	0.7464	–	J_B	0.12	–
α_f	0.00015	–	SFW	858	m^3/h
ρ_O	2.63	t/m^3	V_{sump}	54	m^3
ρ_B	7.84	t/m^3	$SVOL$	35	m^3
P_{mill}	12.6	MW	CFF	3141	m^3/h
P_{max}	14	MW	CFD	1.65	t/m^3
α_{speed}	0.82	–	PSE	0.60	–

4. FLOTATION CIRCUIT MODEL DESCRIPTION

The flotation model of Jämsä-Jounela et al. (2003) gives a very simple way to model the level of flotation cells in series by considering the flow rates into and out of each flotation cell, and is used in this simulation study. The concentrate flow rate is much lower than the tailings flow rate and its effect on the cell level is ignored in this simulation study. The simulated plant has seven flotation cells in series as shown in Fig. 2.

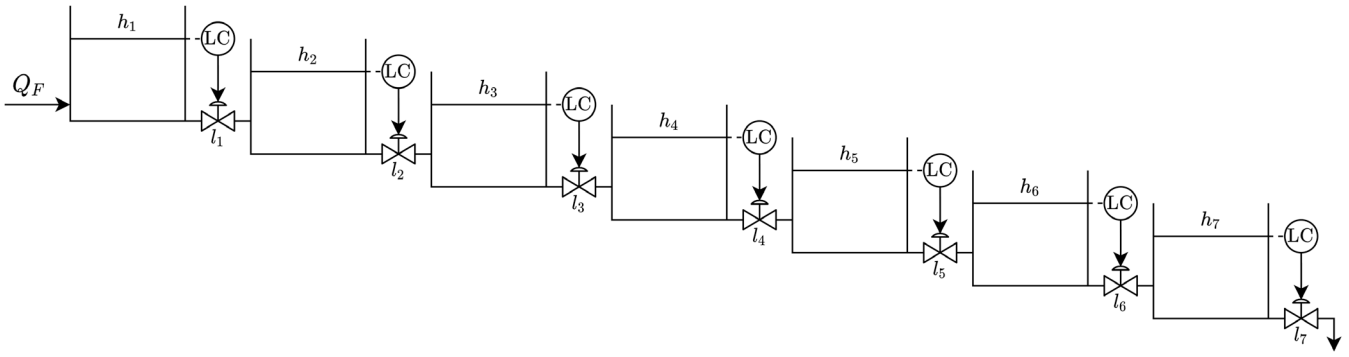

Fig. 2. Flotation bank configuration with regulatory controllers

Table 2. Grinding circuit estimated parameters and initial states.

Parameter	Value	Unit	Parameter	Value	Unit
Mill and feeder parameters					
MFB	50.297	t/h	$\varphi_{P_{max}}$	0.49	–
ε_0	0.6	–	ϕ_r	5.496	kWh/t
δ_{pv}	0.5	–	ϕ_b	90	kWh/t
δ_{ps}	0.5	–	ϕ_f	27.675	kWh/t
χ_P	0	–	α_{ϕ_f}	0.01	–
α_P	0.53	–	d_q	185.09	h^{-1}
$v_{P_{max}}$	0.307	–			
Cyclone parameters					
ε_c	487.228	–	C_3	4	–
C_1	0.6	–	C_4	4	–
C_2	0.7	–	α_{su}	1.099	–
States					
V_{mw}	28.175	m^3	V_{mf}	6.810	m^3
V_{mb}	59.640	m^3	V_{sw}	21.043	m^3
V_{mr}	32.655	m^3	V_{ss}	13.957	m^3
V_{ms}	32.109	m^3	V_{sf}	2.960	m^3

The change in volume of the first cell is,

$$\dot{V}_1 = Q_F - \left(K \cdot C_v \cdot f_c(l_1) \cdot \sqrt{h_1 - h_2 + H_1}\right), \quad (21)$$

where Q_F (m^3/h) is the feed flow rate to the first cell and is equal to the CPF (assuming no storage or conditioning tank is used between the milling and flotation circuits). h_i (m) is the pulp level in the i^{th} cell, H_i (m) is the physical difference in height between cell i and cell $i+1$, K is a constant coefficient, and C_v is the valve capacity coefficient. l_i is the valve control signal of the i^{th} cell and is a value between zero and one with zero being completely closed and one completely open. Linear valves are assumed, therefore $f_c(l_i) = l_i$. For cells 2 to 6 where i is the cell number, the change in volume is,

$$\begin{aligned}\dot{V}_i = &\left(K \cdot C_v \cdot f_c(l_{i-1}) \cdot \sqrt{h_{i-1} - h_i + H_{i-1}}\right) \\ &- \left(K \cdot C_v \cdot f_c(l_i) \cdot \sqrt{h_i - h_{i+1} + H_i}\right),\end{aligned} \quad (22)$$

and for cell 7 the change in volume is,

$$\begin{aligned}\dot{V}_7 = &\left(K \cdot C_v \cdot f_c(l_6) \cdot \sqrt{h_6 - h_7 + H_6}\right) \\ &- \left(K \cdot C_v \cdot f_c(l_7) \cdot \sqrt{h_7 + H_7}\right).\end{aligned} \quad (23)$$

The cross-section of the cells (A_i) are assumed to be constant. The change in pulp levels in the cells is therefore,

$$\dot{h}_i = \frac{\dot{V}_i}{A_i}. \quad (24)$$

The valve capacity coefficient (C_v) is calculated according to the ISA standard (ISA-75.01.01-2007),

$$C_v = 1.17 \cdot Q_m \cdot \sqrt{\frac{\rho_P}{\Delta p}}, \quad (25)$$

where ρ_P is the pulp density (t/m^3). The pressure difference over the valve (Δp) is assumed to be a function of the physical height difference of the cells and pulp density only and is,

$$\Delta p = \rho_P g H_i, \quad (26)$$

where $g = 9.81\ m/s^2$. Q_m is the mean flow rate (m^3/h) through the cell,

$$Q_m = 1.2\frac{V_i}{\tau/60}, \quad (27)$$

where τ (min) is the pulp retention time in the cell.

The flotation model parameters and initial states were obtained from an industrial flotation circuit and are given in Table 3.

Table 3. Flotation circuit parameters and initial states.

Parameter	Value	Unit	Parameter	Value	Unit
Q_F	1519.6	m^3/h	$K_{i=1..6}$	3.076	$m^{2.5}/s$
V_{cell}	76	m^3	K_7	1.074	$m^{2.5}/s$
A_i	12	m^2	h_i	6.123	m
H_i	0.85	m	V_i	73.476	m^3
τ	5	min	l_1	0.5	-

5. SIMULATION

The circuit models are simulated with different disturbances in the grinding circuit to monitor the changes in the levels of the flotation cells. Fig. 3 shows the inputs and the disturbances during the simulation. A step disturbance in ϕ_f of $+10\ kWh/t$ is introduced for 1 hour at $t = 1$ h under normal operating conditions. Then from $t = 3$ h for 1 hour a step disturbance of $+3\ kWh/t$ is introduced in ϕ_r. The first two disturbances simulate an increase in the power needed per tonne of fines and rocks produced respectively. This reflects a change in the hardness of the ore. Spillage water of 10% of SFW is added to the sump from $t = 5$ h for 1 hour and from $t = 7$ h for 1 hour the PSE setpoint is increased by 0.03%. Lastly, the ϕ_f,

ϕ_r as well as the spillage water disturbance are simulated simultaneously from $t = 9$ h for 2 hours.

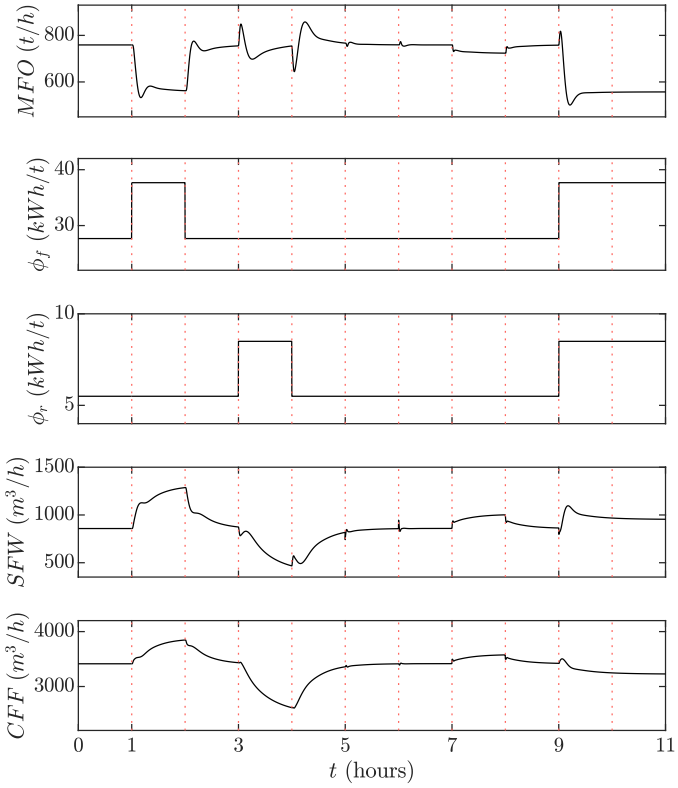

Fig. 3. Grinding circuit input simulation result

A PI-controller is used to regulate the charge inside the mill (J_T) by manipulating the feed ore and water flow rates into the mill (MFO and MIW). The flow rates are controlled in a constant ratio of $MIW/MFO = 0.49$ to ensure that the change in slurry density is kept as small as possible. A second PI-controller is used to control the sump level with the sump feed water (SFW) and a third control the PSE with the CFF. On each of the seven flotation cells a PI-controller is implemented to control the level of the cell to a setpoint of 6.123 m by adjusting the linear valves limiting the outflow of each cell. The PI-controllers have the form,

$$MV(t) = MV(0) + K_c \left(E(t) + \frac{1}{\tau_I} \int_0^t E(t)dt \right) \quad (28)$$

where $E(t) = SP(t) - CV(t)$, MV is the manipulated variable, SP is the setpoint, CV is the controlled variable, and K_c is the proportional gain, and τ_I is integration constant. Table 4 gives the controller parameters for the PI-controllers.

Table 4. PI-controller parameters.

CV	SP	MV	MV(0)	K_c	τ_I
J_T	0.307%	MFO	759 t/h	36365	0.116
$SVOL$	35 m^3	SFW	858 m^3/h	145.5	0.04
PSE	0.6%	CFF	3414 m^3/h	2500	0.08
h_i	6.123 m	l_i	0.5	-1	0.02

The circuit models are simulated in MATLAB and Simulink for 11 hours with a sampling interval of 10 seconds using the Runge-Kutta 4^{th} order numerical integration method. The simulation results of the grinding mill and flotation cells can be seen in Fig. 4 and Fig. 5 respectively.

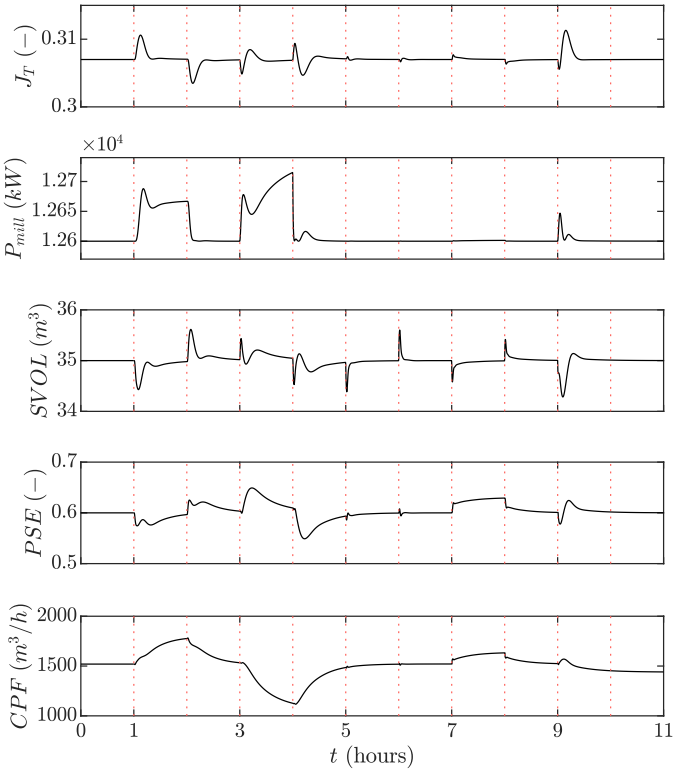

Fig. 4. Grinding circuit output simulation result

6. DISCUSSION AND CONCLUSION

The change in hardness of the ore simulated by the step disturbance in ϕ_f reduces the amount of fines produced which increases the charge in the mill (J_T). The controller adjusts to this change by decreasing the input feed MFO and MIW to keep the charge in the mill at the setpoint. The reduced flow volume into the mill causes a drop in the sump level and thus an increase in SFW as shown in Fig. 3 and Fig. 4. The increase in ore hardness also causes a decrease in PSE for which the controller compensates by increasing CFF. The increased cyclone feed rate results in an increased cyclone outflow and the flotation levels start to rise as shown in Fig. 5. The disturbance in ϕ_r has a similar effect on the mill as the disturbance in ϕ_f, but in the opposite direction. The disturbances in ϕ_f and ϕ_r causes an increase in P_{mill} since more power is used to grind the harder ore.

The effect of the sump spillage water disturbance is negated by the sump level controller which acts quickly by decreasing SFW and bringing the sump level back to the setpoint. The step disturbance in PSE and subsequent increase in CFF to correct it directly affects the cyclone by increasing both the underflow and overflow and a slight increase in the cell levels can be seen. The combination of different disturbances almost cancels each other out since the individual disturbances cause changes in opposite

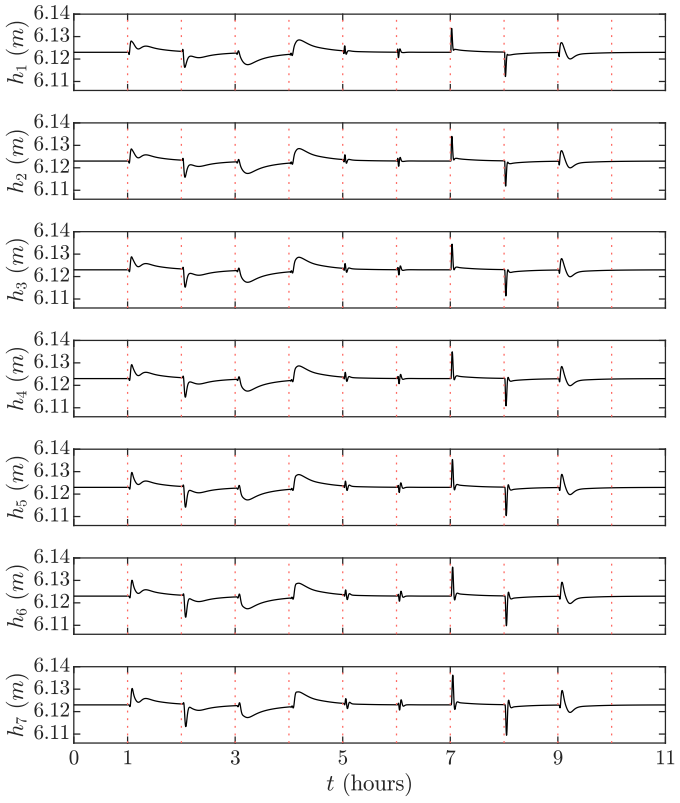

Fig. 5. Flotation bank simulation result

directions and only a small increase in the flotation levels can be seen.

As expected, Fig. 5 shows how the disturbances of the grinding mill circuit propagate through the flotation cells. Although the cell level variations are relatively small, at least in this simulation scenario, it is clear that the effect of the disturbances on CPF propagates from the first cell to the last cell. The disturbance of the ore hardness via ϕ_f and ϕ_r has the largest overall impact on the flotation cell, while the sump spillage water disturbance results in the largest sudden change in the cell levels. It is not visible in this graph, but there is a small delay in the propagation of the disturbance from one cell to the next. It is clear that multivariable control is required to optimally control the flotation levels and prevent the propagation of the disturbance through the flotation cells (Schubert et al., 1995; Smith et al., 2004).

Possible future work can include the effect of the disturbances on the final grade and recovery and not only the cell levels. The model can also be expanded to include a more comprehensive flotation model, such as by Oosthuizen et al. (2021) and validating the plant-wide model with industry data. A better control framework can be designed using an expanded plant-wide model to optimise the economic performance of the plant. Control actions for extreme cases such as a complete stop in ore feed can also be explored and included in the control framework.

ACKNOWLEDGEMENTS

This work is based on research supported by the National Research Foundation of South Africa (Grant number 130380).

REFERENCES

Hodouin, D., Jämsä-Jounela, S.L., Carvalho, M.T., and Bergh, L. (2001). State of the art and challenges in mineral processing control. *Control Engineering Practice*, 9(9), 995–1005.

ISA-75.01.01-2007 (2007). Flow Equations for Sizing Control Valves. Standard, International Society for Automation, North Carolina, USA.

Jämsä-Jounela, S.L., Dietrich, M., Halmevaara, K., and Tiili, O. (2003). Control of pulp levels in flotation cells. *Control Engineering Practice*, 11(1), 73–81.

Jovanović, I. and Miljanović, I. (2015). Contemporary advanced control techniques for flotation plants with mechanical flotation cells - A review. *Minerals Engineering*, 70, 228–249.

Laurila, H., Karesvuori, J., and Tiili, O. (2002). Strategies For Instrumentation and Control of Flotation Circuits. *Mineral Processing Plant Design, Practice and Control*, 2, 2174–2195.

le Roux, J.D. and Craig, I.K. (2019). Plant-Wide Control Framework for a Grinding Mill Circuit. *Industrial and Engineering Chemistry Research*, 58(26), 11585–11600.

le Roux, J.D., Craig, I.K., Hulbert, D.G., and Hinde, A.L. (2013). Analysis and validation of a run-of-mine ore grinding mill circuit model for process control. *Minerals Engineering*, 43-44, 121–134.

McIvor, R.E. and Finch, J.A. (1991). A guide to interfacing of plant grinding and flotation operations. *Minerals Engineering*, 4(1), 9–23.

Muñoz, C. and Cipriano, A. (1999). An integrated system for supervision and economic optimal control of mineral processing plants. *Minerals Engineering*, 12(6), 627–643.

Oosthuizen, D.J., le Roux, J.D., and Craig, I.K. (2021). A dynamic flotation model to infer process characteristics from online measurements. *Minerals Engineering*, 167, 106878.

Schena, G., Casali, A., and Vallebuona, G. (1996). Optimal throughput policies for a copper concentrator. *Minerals Engineering*, 9(11), 1105–1117.

Schubert, J., Henning, R., Hulbert, D., and Craig, I. (1995). Flotation control - a multivariable stabilizer. In *XIX International Mineral Processing Congress*. San Francisco.

Smith, G.C., Jordaan, L., Singh, A., Vandayar, V., Smith, V.C., Muller, B., and Hulbert, D.G. (2004). Innovative process control technology for milling and flotation circuit operations. *Journal of The South African Institute of Mining and Metallurgy*, 104(6), 353–365.

Sosa-Blanco, C., Hodouin, D., Bazin, C., Lara-Valenzuela, C., and Salazar, J. (2000). Economic optimization of a flotation plant through grinding circuit tuning. *Minerals Engineering*, 13(10), 999–1018.

Thivierge, A., Bouchard, J., Desbiens, A., and Pérez, E.M. (2019). Modeling the product net value of a grinding-flotation circuit. *IFAC-PapersOnLine*, 52(14), 18–23.

Wei, D. and Craig, I.K. (2009a). Economic performance assessment of two ROM ore milling circuit controllers. *Minerals Engineering*, 22(9-10), 826–839.

Wei, D. and Craig, I.K. (2009b). Grinding mill circuits - A survey of control and economic concerns. *International Journal of Mineral Processing*, 90(1-4), 56–66.